



Molecular Crystals and Liquid Crystals Science and Technology. Section A. Molecular Crystals and Liquid Crystals

Publication details, including instructions for authors and
subscription information:

<http://www.tandfonline.com/loi/gmcl19>

Molecular and Crystal Structure and Properties of Te-Containing p- Terphenoquinone Analogues

Rui Tamura ^a, Mroyuki Takasuka ^b, Yuya Nagata ^b, Nagao Azuma
^b, Akira Matsumoto ^b, Yoshihiko Sadaoka ^c, Atsushi Gunji ^d,
Kazuko Takahashi ^d, Akio Kamimura ^e & Kenzi Hori ^e

^a Laboratory of Organic Chemistry, Division of Material Science,
Graduate School of Environmental Earth Science, Hokkaido
University, Sapporo, 060, Japan

^b Department of Chemistry, Faculty of General Education, Ehime
University, Matsuyama, 790, Japan

^c Department of Applied Chemistry, Faculty of Engineering,
Ehime University, Matsuyama, 790, Japan

^d Department of Chemistry, Faculty of Science, Tohoku
University, Sendai, 980, Japan

^e Department of Chemistry, Faculty of Liberal Arts, Yamaguchi
University, Yamaguchi, 753, Japan

Version of record first published: 24 Sep 2006.

To cite this article: Rui Tamura , Mroyuki Takasuka , Yuya Nagata , Nagao Azuma , Akira
Matsumoto , Yoshihiko Sadaoka , Atsushi Gunji , Kazuko Takahashi , Akio Kamimura & Kenzi Hori
(1996): Molecular and Crystal Structure and Properties of Te-Containing p-Terphenoquinone
Analogues, Molecular Crystals and Liquid Crystals Science and Technology. Section A. Molecular
Crystals and Liquid Crystals, 278:1, 139-150

To link to this article: <http://dx.doi.org/10.1080/10587259608033666>

PLEASE SCROLL DOWN FOR ARTICLE

Full terms and conditions of use: <http://www.tandfonline.com/page/terms-and-conditions>

This article may be used for research, teaching, and private study purposes. Any substantial or systematic reproduction, redistribution, reselling, loan, sub-licensing, systematic supply, or distribution in any form to anyone is expressly forbidden.

The publisher does not give any warranty express or implied or make any representation that the contents will be complete or accurate or up to date. The accuracy of any instructions, formulae, and drug doses should be independently verified with primary sources. The publisher shall not be liable for any loss, actions, claims, proceedings, demand, or costs or damages whatsoever or howsoever caused arising directly or indirectly in connection with or arising out of the use of this material.

MOLECULAR AND CRYSTAL STRUCTURE AND PROPERTIES OF Te-CONTAINING *p*-TERPHENOQUINONE ANALOGUES

RUI TAMURA,^{*1} HIROYUKI TAKASUKA,² YUYA NAGATA,² NAGAO
AZUMA,² AKIRA MATSUMOTO,² YOSHIHIKO SADAOKA,³ ATSUSHI
GUNJI⁴, KAZUKO TAKAHASHI,⁴ AKIO KAMIMURA⁵ AND KENZI
HORI⁵

¹Laboratory of Organic Chemistry, Division of Material Science, Graduate School
of Environmental Earth Science, Hokkaido University, Sapporo 060, Japan,

²Department of Chemistry, Faculty of General Education and ³Department of
Applied Chemistry, Faculty of Engineering, Ehime University, Matsuyama 790,
Japan, ⁴Department of Chemistry, Faculty of Science, Tohoku University, Sendai
980, Japan and ⁵Department of Chemistry, Faculty of Liberal Arts, Yamaguchi
University, Yamaguchi 753, Japan

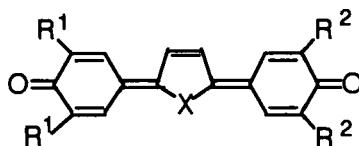
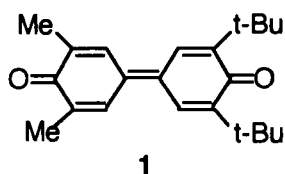
Abstract *p*-Terphenyloquinone analogues containing a quinonoid type of
tellurophene skeleton in the central position have been prepared with a view to
developing a new type of organic photoconductive materials having amphoteric
redox properties. X-ray structure analysis showed that each molecule exhibited
an asymmetric boat conformation owing to the bent structure of the whole ring
system and the opposite twisting of two terminal rings. The molecular packing
manner in the crystals depends on the substituents on the terminal quinonoid
rings. These compounds were electrically amphoteric and afforded radical cation
salts and CT complexes by electrochemical or chemical oxidation or by the
reaction with an appropriate electron acceptor, respectively. Preliminary
experimental results on the photoconductive properties of the neutral compound
along with the electrical and magnetic properties of the radical cation salts and CT
complexes are described.

INTRODUCTION

Photoconductive materials are the key component for designing photoelectrochemical
devices such as solar cells and electrophotographic printing systems. Particularly,
development of organic photoconductive materials have been closely associated with the
progress in electrophotography, in which the original simple single-layer photoreceptors
have been replaced by bilayer photoreceptor devices consisting of the charge-generation
layer (CGL) and the charge-transporting layer (CTL) to satisfy demanding requirements
such as high quantum efficiency of photogeneration, a high charge mobility across the
device and a good mechanistic strength.¹ Since the technology of hole-transporting
materials consisting of polymeric films doped with electron donors such as aromatic
amines and hydrazones is more advanced than that of electron-transporting ones, to

date most of practical bilayer organic photoreceptors are negatively corona-charged at the surface on the upper hole-transporting layer. However, the use of the negative corona-charging mode is always accompanied by two indispensable disadvantages; the insufficient discharge stability and the considerable generation of ozone gas harmful to both human and photoreceptors. Therefore, development of positively corona-charged organic photoreceptor devices is desired from the economical and environmental standpoints. It has been disclosed that unsymmetrical diphenoquinone **1** has sufficient electron affinity, exhibits high chemical stability of the resulting radical anion species and excellent electron-transporting ability, and shows high solubility in organic solvents and high dispersibility in binder polymers mainly due to the less cohesive force between the molecules.² However, it is more desirable if single-layered polymeric films doped with both electron donors and acceptors³ or more ideally with single component having amphoteric redox properties can possess the sufficient bipolar charge transporting ability in the positively surface-charged fashion, compared with the bilayer systems described above.

Electrically amphoteric five-membered heterocycle-extended quinones, tetrasubstituted *p*-terphenylquinone analogues **2**,⁴ **3**,⁵ and **5**⁶ synthesized recently by us might be promising candidates for single layered photoelectrochemical devices, because (1) they are fairly stable molecules both in the solid state and in solution, (2) they may retain essentially a coplanar conformation for the whole molecule like **3c**^{5b}, (3) they exhibit an intense π - π^* absorption maximum in the visible wave length region (550 - 600 nm),^{5,6} (4) a fine adjustment of the HOMO-LUMO energy split might be possible by judicious choice of the central five-membered heterocycle and the substituents at the α -positions of the carbonyl groups in the terminal quinonoid rings,^{5c} (5) they are both reducible and oxidizable through multistage electron-transfer reactions,^{4,5,6} (6) they may not easily form CT-complexes with electron donors, (7) the corresponding radical anions and the dianions are fairly stable in solution, owing to the existence of the heteroatom in the central ring,^{4,5,6} and (8) the corresponding radical cations, which must be more



- 2:** X=O **a:** R¹=R²=H
3: X=S **b:** R¹=R²=Me
4: X=Se **c:** R¹=R²=t-Bu
5: X=Te **d:** R¹=Me, R²=t-Bu

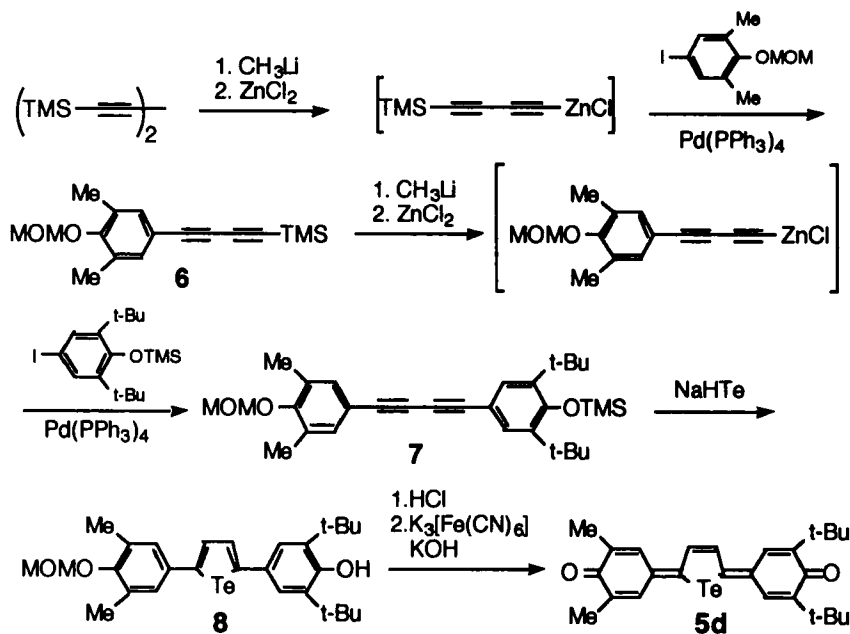
stable in the solid state than in solution, can be stabilized by changing the central heteroatom (O, S, Se and Te) and the substituents on the terminal quinonoid rings.

Tellurium-containing *p*-terphenoquinone analogues **5b** showed very low oxidation potential (Table II) and fairly high electrical conductivities in its radical cation salts.⁶ However, it exhibited intractable poor solubility in organic solvents, probably due to strong intermolecular Te---Te contacts and π - π stacking leading to the aggregation, strictly prevented further application. Therefore, we focused on dissymmetrically substituted **5d** that would have the reduced cohesive force between molecules resulting in improvement of solubility in organic solvents. We here describe the synthesis, structural analysis and electrochemical properties of **5d**, together with preliminary experimental results on the photoconductive properties of **5d** and the electrical and magnetic properties of the CT complex and radical cation salt derived from **5d**.

PREPARATION OF Te-CONTAINING *p*-TERPHENOQUINONE ANALOGUE (5d)

The synthetic procedure of **5d** is shown in Scheme 1. To a solution of 1,4-bis(trimethylsilyl)-1,3-butadiyne (0.970 g, 5.00 mmol) in THF (5 mL) was added dropwise MeLi (1.05 M ether solution, 5.24 mL, 5.50 mmol) at -78°C under argon atmosphere, followed by warming to 25°C over 1 h and additional stirring for 2 h at 25°C. A solution of anhydrous ZnCl₂ (0.780 g, 5.5 mmol) in THF (5 mL) was added to the resulting mono lithium acetylide solution and the mixture was stirred for 2 h at 25°C. This solution was then transferred to a mixture of 2,6-dimethyl-4-iodo-1-methoxymethoxybenzene (1.62 g, 5.50 mmol) and Pd(PPh₃)₄ (0.280 g, 0.25 mmol) in THF (5 mL) at 25°C and the reaction mixture was stirred overnight at 25°C. Water (30 mL) was added, and the aqueous mixture was extracted with ether (3 x 30 mL). The combined organic phase was dried over MgSO₄, and concentrated in vacuo. The residual black oil was passed through short-path silica gel column (hexane) to give 0.972 g (68%) of oily crude **6**: ¹H NMR (CDCl₃) δ 6.98 (s, 2H), 4.95 (s, 2H), 3.55 (s, 3H), 2.22 (s, 6H), 0.22 (s, 9H).

MeLi (3.57 mL, 3.40 mmol) was added dropwise to a solution of the crude **6** (0.974 g, 3.40 mmol) in THF (5 mL) at -78°C under Ar, and the mixture was warmed to 25°C over 1 h and stirred for 2 h at 25°C. A solution of anhydrous ZnCl₂ (0.423 g, 3.40 mmol) in THF (5 mL) was added to the resulting lithium acetylide solution and the mixture was stirred for 2 h at 25°C. This solution was then transferred to a mixture of 2,6-di-*t*-butyl-4-iodo-1-(trimethylsilyloxy)benzene (2.02 g, 5.00 mmol) and Pd(PPh₃)₄

SCHEME 1 Preparation of **5d**.

(0.173 g, 0.15 mmol) in THF (5 mL) at 25°C and the reaction mixture was stirred overnight at 25°C. By a similar workup procedure described above, 1.20 g (72%) of crude **7** was obtained as an oil. **7**: ^1H NMR (CDCl_3) δ 7.43 (s, 2H), 7.33 (s, 2H), 5.01 (s, 2H), 3.63 (s, 3H), 2.23 (s, 6H), 1.34 (s, 18H), 0.33 (s, 9H).

A solution of the crude **7** (0.815 g, 1.66 mmol) in benzene (5 mL) was added all at once to the hot NaHTe solution prepared by refluxing a mixture of powdered tellurium (0.635 g, 4.98 mmol) and NaBH_4 (0.440 g, 11.6 mmol) in EtOH (20 mL) for 1 h, and the reaction mixture was refluxed overnight and then cooled to 25°C. The solvent was removed in vacuo and the residual solid was extracted with CH_2Cl_2 (3 x 20 mL). The combined extracts were filtered and concentrated to give the crude **8** as a yellow powder. To the crude **8** (0.437 g, 0.797 mmol) in THF (8 mL) was added conc HCl (0.2 mL), and the mixture was stirred for 5 h at 50°C. After cooling to 25°C, 0.1N aq KOH solution (40 mL) and $\text{K}_3[\text{Fe}(\text{CN})_6]$ (1.05 g, 3.19 mmol) was added and the reaction mixture was stirred overnight at 25°C. Water (30 mL) was added, and the aqueous mixture was extracted with CH_2Cl_2 (3 x 30 mL). The combined organic phase was dried over MgSO_4 , and concentrated in vacuo to give 0.291 g of crude **5d** as a dark blue powder. Purification by column chromatography on silica gel (20:1 hexane/ethyl acetate) followed by recrystallization from hexane gave 0.175 g (21 % from **7**) of

analytically pure **5d**: mp 189.5-191.5°C; IR (KBr) 2954, 1589, 1499, 1357, 1199, 1031 cm⁻¹; UV-vis (CH₂Cl₂) λ_{max} nm (log ε) 355 sh (3.48), 434 (4.04), 448 (4.04), 482 sh (3.77), 591 (4.52). ¹H NMR (CDCl₃) δ 7.83 (d, J= 6.4Hz, 1H), 7.78 (d, J=6.4Hz, 1H), 7.54 (dd, J=2.6, 1.3Hz, 1H), 7.52 (d, J=2.6Hz, 1H), 6.77 (dd, J=2.6, 1.4Hz, 1H), 6.66 (d, J=2.6Hz, 1H), 2.10 (d, J=1.2Hz, 3H), 2.13 (d, J=1.2Hz, 3H), 1.36 (s, 9H), 1.33 (s, 9H); ¹³C NMR (CDCl₃) δ 186.9, 185.9, 151.0, 150.9, 150.4, 147.0, 141.5, 141.1, 138.6, 137.8, 135.9, 135.5, 134.9, 134.6, 127.6, 124.0, 35.6, 35.5, 29.6, 29.5, 16.8, 16.7. Anal. Calcd for C₂₆H₃₀O₂Te: C, 62.19; H, 6.02. Found: C, 62.51; H, 6.09.

5d showed high solubility in most organic solvents.

MOLECULAR AND CRYSTAL STRUCTURES OF *p*-TERPHENOQUINONE ANALOGUE (**5c** and **5d**)

The single crystals of **5c** and **5d** of good quality for X-ray crystallographic analysis were obtained by recrystallization from acetone and hexane, respectively, whereas attempted recrystallization of **5b** from various solvents failed to produce the single crystal, giving only powder. The crystals of **5c** were red-brown blocks, while **5d** black needles. The crystal data for **5c** and **5d** summarized in Table I show that each molecule in the crystals of both **5c** and **5d** has chirality. Although **5c** and **5d** essentially retain a coplanar conformation for the whole molecule, they exhibit the slight boat conformation with dihedral angles of 8.8° and -3.6° (Figure 1a), and 1.9° and -5.7° (Figure 2a), respectively, between the mean plane of the central five-membered ring and each mean plane of the two terminal six-membered rings. Therefore, the dihedral angles between the mean planes of the two terminal six-membered rings for **5c** and **5d** are 10.3° and 7.2°, respectively. This boat conformation and the opposite twisting of the two terminal six-membered rings to the central five-membered ring with twisting angles of 5° and 8°, and 2° and 9° for **5c** and **5d**, respectively, (and dissymmetrical substitution in the case of **5d**) would be responsible for the molecular chirality observed in the crystal state. The boat conformation of **5c** is in contrast to the chair conformation observed for the corresponding sulfur-analogue **3c**,^{5b} where the mean planes of the terminal six-membered rings incline 9.1° and 11.1°, respectively, from that of the central five-membered ring and hence the twisting angle between the mean planes of the two terminal rings is 1.8°. Furthermore, it has been found that **5c** is composed of enantiomerically pure crystals, while the crystals of **5d** and **3c** were racemic in the crystallographic sense.

As to the crystal structure, **5d** has the distinct molecular stacking along the *a* axis with alternate intermolecular face-to-face distances of 3.6 and 3.8 Å (Figure 2b), although short intermolecular Te---Te contacts are not observed because of the alternate stacking of two enantiomers oppositely directed to each other so as to avoid the steric hindrance between di-*t*-butyl-substituted six-membered rings. Therefore, the observed intermolecular interaction in the crystal of **5d** is one-dimensional in this direction. On the other hand, no noticeable intermolecular interaction was observed in **5c** and the shortest intermolecular face-to-face distance of **5c** was as long as 10 Å, the length of the *b* axis (Figure 1b).

TABLE I Selected crystallographic parameters for **5c** and **5d**.

	5c	5d
space group	<i>P</i> 2 ₁	<i>P</i> 2 ₁ /c
<i>a</i> , Å	9.446 (2)	8.095 (2)
<i>b</i> , Å	10.259 (2)	18.103 (2)
<i>c</i> , Å	17.750 (3)	16.493 (2)
β	91.26 (1)	103.46 (1)
<i>Z</i>	2	4
R/Rw	0.040/0.037	0.040/0.037

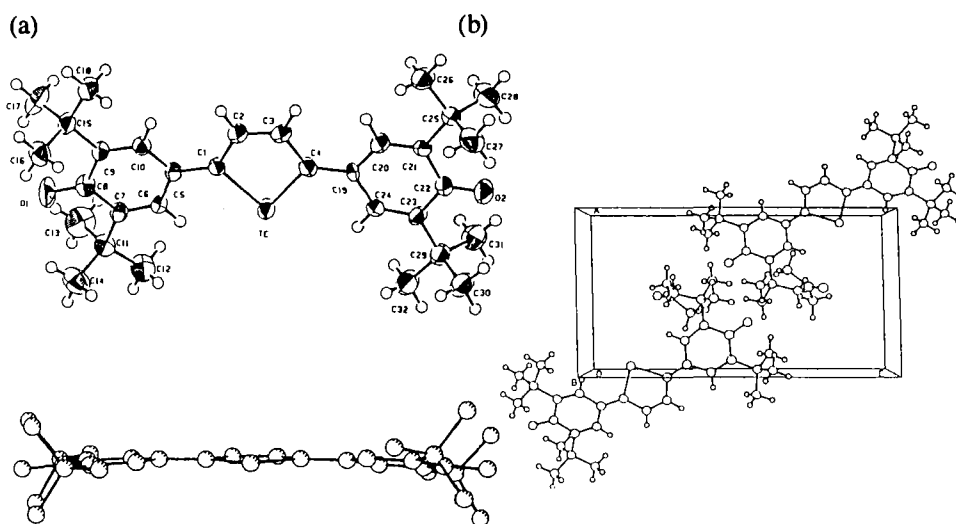
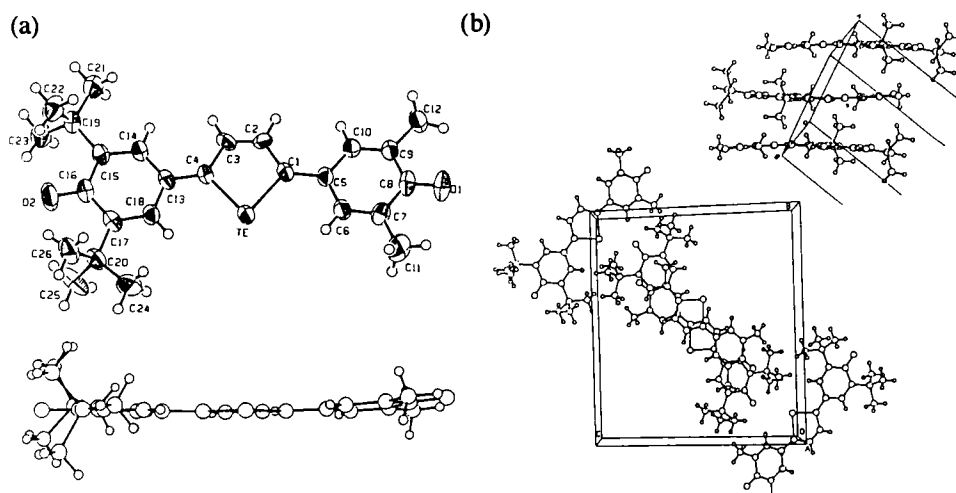


FIGURE 1 (a) Molecular and (b) crystal structure of **5c**.

FIGURE 2 (a) Molecular and (b) crystal structure of **5d**.

Thus, it is concluded that from the crystal data **5d** seems to be superior to **5c** as a conducting material.

ELECTROCHEMICAL PROPERTIES AND UV-VIS ABSORPTION SPECTRA

The cyclic voltammogram of **5d** in benzonitrile exhibited two reversible reduction waves with half-wave reduction potentials of -0.57 and -0.74V and an irreversible oxidation

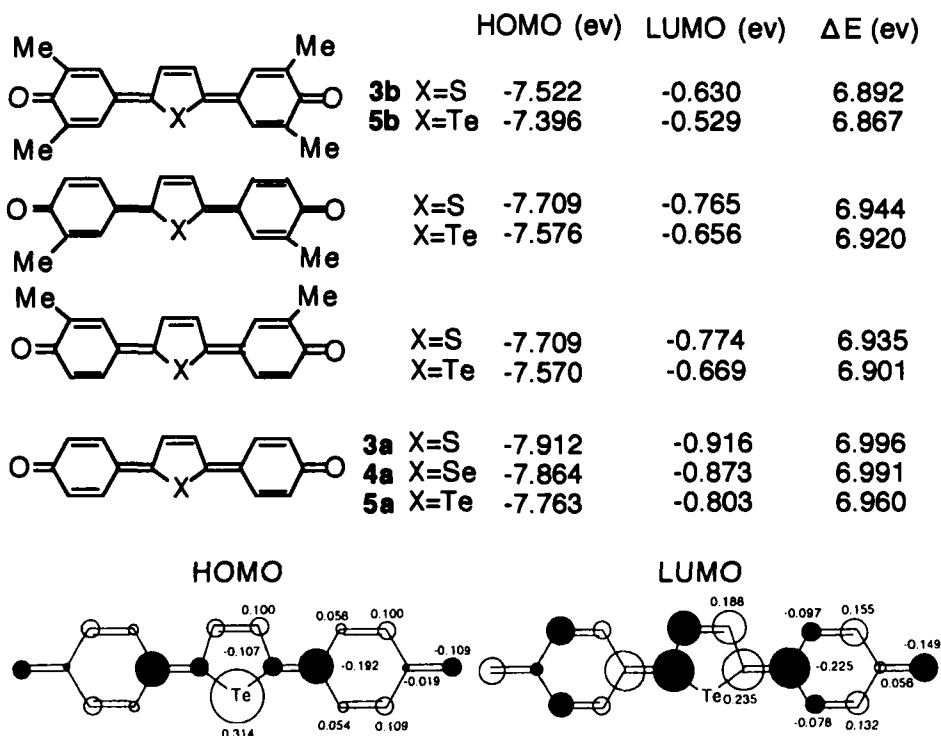
TABLE II Redox potentials and UV-vis spectra of **1**, **3**, **4** and **5**.^a

Compd.	Solvent	E_{1}^{red}	E_{2}^{red}	$E_{\text{pa}}^{\text{ox}}$	E_{1}^{sum}	λ_{max} [nm] (loge)
1	CH ₂ Cl ₂	-0.48	-	-	-	422 (5.20) ^j
3b , ^{b,c}	PhCN	-0.37	-0.44	1.24 ^f	1.61	546 (4.87) ^{c,i}
3c , ^{b,c}	PhCN	-0.47	-0.67	1.28 ^g	1.75	558 (4.90) ^{c,i}
5b ^d	PhCN	-0.68 ^e		0.63 ^h	1.31	592 (4.47) ^{d,j}
5c ^d	PhCN	-0.59	-0.73	1.04 ^h	1.63	593 (4.79) ^{d,j}
5d	PhCN	-0.57	-0.74	1.15 ^f	1.72	591 (4.52) ^j

^a Potentials (V vs. SCE) were measured by CV with 0.1 M (n-Bu)₄NClO₄ at 25°C (scan rate, 50 mV/s). $E_{\text{pa}}^{\text{ox}}$ is measured based on the anodic peak current. $E_{1}^{\text{sum}} = E_{\text{pa}}^{\text{ox}} - E_{1}^{\text{red}}$. ^b 0.1M (n-Bu)₄NBF₄ was employed for CV measurement. ^c Cited from ref 5b. ^d Cited from ref 6. ^e Two electron reduction. ^f Irreversible. ^g Reversible. ^h Quasi-reversible. ⁱ Measured in CH₃CN. ^j Measured in CH₂Cl₂.

wave with an oxidation peak at 1.15V vs SCE electrode (Table II). The oxidation potential of **5d** is similar to that of **5c**, but quite different from that of **5b**. The reduction behaviour of **5d** is also similar to that of **5c** showing two-step one-electron reduction potentials. The reduction potentials of **5d** is more negative by ca 0.1V than those of **1** and **3c**.

Ab initio frontier molecular orbital calculations of unsubstituted charco-gen-containing *p*-terphenylquinone analogues **3a**, **4a** and **5a** indicate that the energy level of the LUMO of the tellurium-analogue is higher than those of the corresponding sulfur and selenium analogues. However, the energy difference between the HOMO and LUMO levels in tellurium-analogue **5a** ($\Delta E=6.960$ eV) is slightly smaller than those of sulfur-analogue **3a** (6.996 eV) and selenium-analogue **4a** (6.991 eV) by the virtue of the relatively high HOMO level ascribing to the low valence state ionization potential of tellurium as shown in Scheme 2.⁷ Furthermore, it is also noteworthy that placing methyl groups on the four α -positions of the carbonyl groups in the terminal quinonoid rings induces the more increase of the HOMO level due to the electron-releasing effect of



SCHEME 2 HOMO and LUMO levels of **3**, **4** and **5** and MO coefficients of **5a**.

methyl groups than that of the LUMO level, eventually resulting in the decrease of the energy difference between the two levels, i.e., **3b** ($\Delta E=6.892$ eV) and **5b** (6.867 eV) (Scheme 2).

In accord with the MO calculations, **5d** showed a lower oxidation potential by 0.09 and 0.13 V and the longer wavelength of the first excitation absorption maximum by 45 and 33 nm than **3b** and **3c**, respectively. This high electron-donating ability of **5d** is mainly ascribed to the low valence state ionization potential of tellurium, since the extent of π delocalization of the $5p\pi$ electrons on the tellurium atom through carbon framework stabilizing the corresponding radical cation is considered to be low because of the disparate size of the tellurium and carbon.⁹ Since the largest MO coefficient resides on the central tellurium atom in the HOMO of **5a** as shown in Scheme 2, the unpaired electron should be localized considerably on the tellurium atom in the radical cation of **5**.

PHOTOCONDUCTIVE PROPERTIES OF 5d

Since **5d** showed high dispersibility in binder polymers such as poly(4,4'-cyclohexylidenediphenyl carbonate (PC-Z) and poly(N-vinylcarbazole) (PVK) as well as high solubility in various organic solvents, preliminary measurements of the photoconductive properties of **5d** were performed. The HOMO and LUMO energy diagram of **5b**, **5c** and **5d** in the solid state was obtained by measuring the ionization potentials of the powdered materials by means of a photoionization method and by calculating the energy gap between the HOMO and LUMO levels from the absorption tails in the electronic spectra of thin films of the materials dispersed in PCZ, as shown in Figure 3. Apparently both the HOMO and LUMO levels of **5d** shows the intermediate values between **5b** and **5c**. From this diagram it is expected that the ionization potential of **5d** is low enough to release an electron by photoirradiation, and this feature might include both the charge separation and transfer between the same molecules. Therefore, in order to evaluate the single-component bipolar charge transporting ability of **5d** upon photoirradiation, the time-of-flight measurement of **5d** dispersed (50 wt %) in PC-Z was attempted by using a nitrogen laser pulse.^{2b} As a result, the single-component of **5d** did not show either of the electron-transport nature or the hole-transport nature in this experiment. Further studies with the aim of designing molecules having amphoteric redox properties so as to induce both the charge separation and transport between the same molecules upon photoirradiation are under investigation.

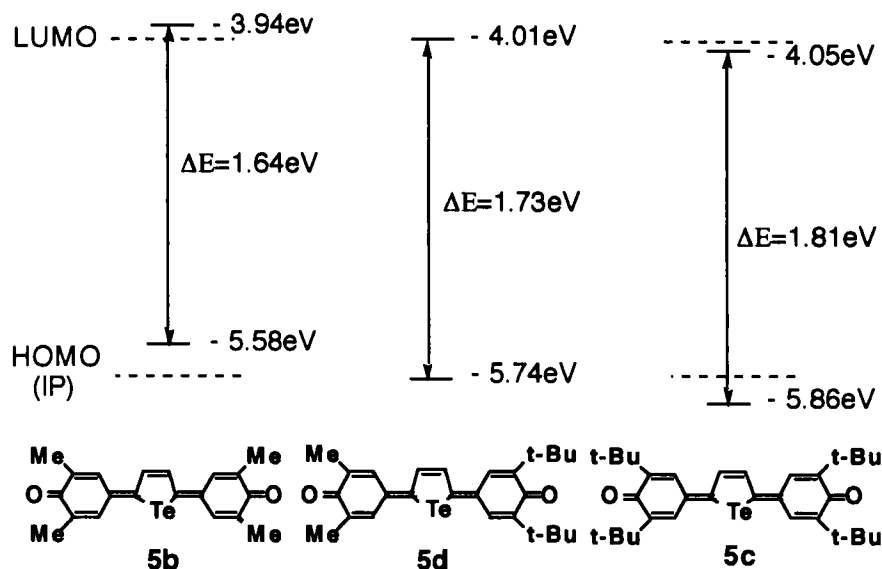


FIGURE 3 Energy diagram of **5b**, **5c** and **5d** in the solid state.

MAGNETIC AND ELECTRICAL PROPERTIES OF RADICAL CATION SALTS AND CT-COMPLEXES

In order to evaluate the electron-donating ability of **5d** and the stability of its radical cation species, the radical cation salt and CT complex of **5d** were prepared by chemical oxidation or by the reaction with an appropriate electron acceptor, respectively. Although electrochemical oxidation of **5d** failed to give any radical cation salt, chemical oxidation of **5d** with (p-BrC₆H₄)₃NSbCl₆¹⁰ provided a radical cation salt, **5d**·[SbCl₆]_{1.2}, in CH₂Cl₂ as a dark black powder. The black powdered CT complex **5d**·TCNQF₄ was also prepared by the reaction of **5d** with TCNQF₄ in hot CH₂Cl₂. Their ESR spectra in the solid state were shown in Figure 4. Although these radical species were fairly stable in the solid state under argon atmosphere, these solution in organic solvents did not exhibit ESR spectra. The radical cation salts **5d**·[SbCl₆]_{1.2} and **5d**·TCNQF₄ were insulators, exhibiting conductivities less than 10⁻⁸ S cm⁻¹ measured by the two-probe method on compressed pellets.

In contrast, radical cation salts of **5b** prepared by the electrochemical oxidation and powdered CT complex **5b**·TCNQF₄ showed higher conductivities of $\sigma \sim 10^{-4}$ and 10⁻⁵ S cm⁻¹, respectively.⁶ The radical cation **5b**·[SbCl₆]_{0.5} prepared by chemical

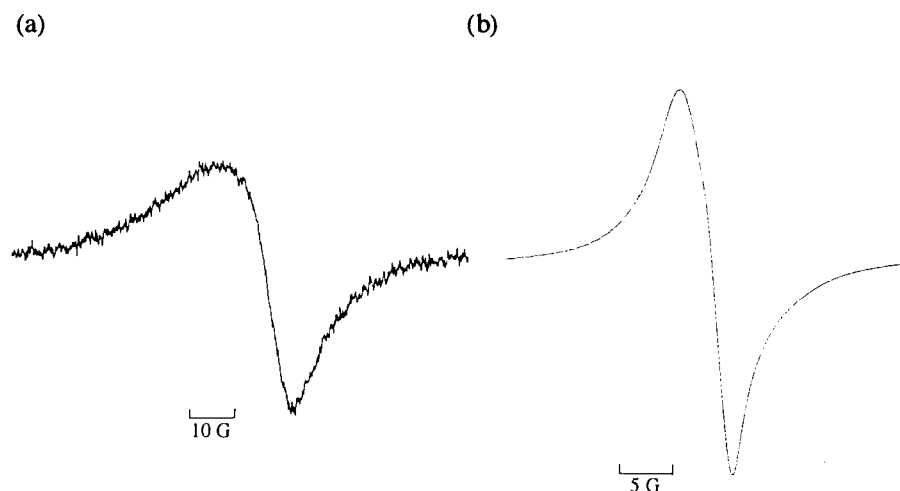


FIGURE 4 ESR spectrum of (a) **5d**·[SbCl₆]_{1.2} and (b) **5d**·TCNQF₄ in the solid state.

oxidation was again an electrical insulator, although the ESR spectra of this radical cation salt was observed ($g=2.0037$, $\Delta H=8.7G$). These results are summarized in Table III. Thus, it is noted that although the radical cation salts are uniformly stable in the solid state, the electrical conductivity of these salts are highly dependent on the manner of preparation and the structure of the **5**.

TABLE III Electrical conductivity and ESR spectral data of radical cation salts and CT complexes derived from **5b** and **5d** in the solid state.^a

Compd.	Conductivity σ (S cm ⁻¹)	<i>g</i> -Value	ΔH (gauss)
5d ·[SbCl ₆] _{1.2} ^b	$< 1.0 \times 10^{-8}$ ^d	2.0038	16.2
5d ·TCNQF ₄ ^b	$< 1.0 \times 10^{-8}$ ^d	2.0033	4.7
5b ·[SbCl ₆] _{0.5} ^b	$< 1.0 \times 10^{-8}$ ^d	2.0037	8.7
5b ·TCNQF ₄ ^b	1.15×10^{-5} ^e	2.0035	5.4
5b ·[BF ₄] ₂ ^c	1.13×10^{-4} ^e	2.0021	11.1
5b ·[ClO ₄] _{1.1} ^c	1.53×10^{-4} ^e	2.0020	10.1
5b ·PF ₆ ^c	1.53×10^{-4} ^e	2.0020	13.4

^a Measured at 25°C. ^b Obtained by the reaction with (p-BrC₆H₄)₃NSbCl₆ in CH₂Cl₂ at 25°C. ^c Obtained by electrochemical oxidation, see ref 6. ^d Measured by two probe method. ^e Measured by four probe method, see ref 6.

ACKNOWLEDGMENT

We thank Prof Masaaki Yokoyama, Osaka University, for various measurements for photoconductive properties. We also thank the Computer Center, Institute for Molecular Science at the Okazaki National Research Institute, Japan, for the use of the HITAC M-600 and S-820/80 computers.

REFERENCES

1. (a) K-y. Law, Chem. Rev., **93**, 449 (1993). (b) P. M. Borsenberger and D. S. Weiss, Organic Photoreceptors for Imaging Systems (Marcel Dekker, New York, 1993).
2. (a) Y. Yamaguchi, H. Tanaka and M. Yokoyama, J. Chem. Soc., Chem. Commun., 222 (1990). (b) Y. Yamaguchi and M. Yokoyama, Chem. Mater., **3**, 709 (1991).
3. Y. Yamaguchi, T. Fujiyama, H. Tanaka and M. Yokoyama, Chem. Mater., **2**, 341 (1990).
4. K. Takahashi, A. Gunji and K. Akiyama, Chem. Lett., 863 (1994).
5. (a) K. Takahashi and T. Suzuki, J. Am. Chem. Soc., **111**, 5483 (1989). (b) K. Takahashi, T. Suzuki, K. Akiyama, Y. Ikegami and Y. Fukazawa, J. Am. Chem. Soc., **113**, 4576 (1991). (c) K. Takahashi and T. Sakai, Chem. Lett., 157 (1993).
6. (a) R. Tamura, Y. Nagata, H. Shimizu, A. Matsumoto, N. Ono, A. Kamimura and K. Hori, Adv. Mater., **5**, 719 (1993).
7. The MO calculations were performed using the LANL1DZ basis set⁸ in the Gaussian 90 program. The geometries were optimized with C_{2v} symmetry (all geometrical parameters were fully optimized).
8. (a) P. J. Hay, W. R. Wadt, J. Chem. Phys., **82**, 270 (1985). (b) W. R. Wadt, P. J. Hay, ibid., **82**, 284 (1985). (c) P. J. Hay, W. R. Wadt, ibid., **82**, 299 (1985).
9. (a) K. A. Lerstrup and L. Henriksen, J. Chem. Soc., Chem. Commun., 1102 (1979). (b) M. Renson, in The Chemistry of Organic Selenium and Tellurium Compounds, Vol. 1, edited by S. Patai and Z. Rappoport (Wiley, 1986), Chap. 13, pp. 399-516.
10. F. A. Bell, A. Ledwith and D. C. Sherrington, J. Chem. Soc. (c), 2719 (1969).